Electronic Supplementary Information for:

High Thermal and Chemical Stability in Pyrazolate-Bridged Metal-Organic Frameworks with Exposed Metal Sites

Valentina Colombo,[a,b,c] Simona Galli,[c] Hye Jin Choi,[a,b] Ggoch Ddeul Han,[a,b] Angelo Maspero,[c] Giovanni Palmisano,[c] Norberto Masciocchi,[c] and Jeffrey R. Long*[,a,b]

[a]*Department of Chemistry, University of California, Berkeley, California 94720, USA. E-mail: jrlong@berkeley.edu*
[b]*Materials Sciences Division, Lawrence Berkeley National Laboratory, Berkeley, California 94720, USA.*
[c]*Dipartimento di Scienze Chimiche e Ambientali, Università dell'Insubria, via Valleggio 11, I-22100 Como, Italy.*

Chem. Sci.

Experimental Details

1,3,5-tris(1*H*-pyrazol-4-yl)benzene (H_3BTP). This compound was synthesized according to the scheme presented in Figure S1. The first intermediate, 1,3,5-benzenetriacetic acid, was prepared from 1,3,5-triacetyl benzene following a procedure described previously.[1a] If necessary, recrystallization of the sample was carried out in acetic acid (65% isolated yield). ^{1}H NMR δ 3.52 (s, 2H), 7.03 (s, 1H), 12.32 (br s, 1H). Anal. Calcd. for $C_{12}H_{12}O_6$ (Mw = 252.20 g/mol): C, 57.14; H, 4.80. Found: C, 56.92; H, 4.82.

The second intermediate, 1,3,5-tris(1-dimethylamino-3-dimethylimonio-prop-1-en-2-yl)benzene tris(perchlorate),[1b] was synthesized using a modification of a previously reported procedure for the synthesis of other 4-aryl-substituted pyrazoles.[2] Under a nitrogen atmosphere, $POCl_3$ (10 mL, 0.11 mol) was added dropwise to anhydrous DMF (40 mL, 0.52 mol) cooled in an ice bath. Then, 1,3,5-benzenetriacetic acid (3 g, 0.0119 mol) was added and the mixture was heated at 90 °C for 18 h. The reaction mixture was then quenched by pouring it into ice water (50 mL) and a saturated aqueous solution of $NaClO_4$ (13.4 g) was added. The yellowish solid was collected by filtration and washed with cold water to afford 6.98 g (78%) of the tris(perchlorate) intermediate. ^{1}H NMR δ 2.60 (br s, 6H), 3.28 (br s, 6H); 7.28 (s, 1H); 7.76 (s, 2H). Anal. Calcd. for $C_{27}H_{45}Cl_3N_6O_{12}$ (Mw = 752.04 g/mol): C, 43.12; H, 6.03; N, 11.17. Found: C, 43.92; H, 5.59; N, 11.65.

The tris(perchlorate) salt (6.98 g, 0.0093 mol) was suspended in a mixed solution of ethanol (100 mL) and water (30 mL) and hydrazine monohydrate (1.44 mL, 0.0297 mol) was added to the mixture. After heating at reflux for 2 h, the mixture was filtered and the residue was washed with methanol (3 × 10 mL) and dried under vacuum to afford 1.74 g (68%) of H_3BTP as a light yellow solid. ^{1}H NMR δ 7.68 (s, 1H); 8.26 (br s, 2H); 12.94 (br s, 1H). IR (neat) 3164(br), 2941(br), 1605(vs), 1371(w), 1348(w), 1232(w), 1158(s), 1044(s), 994(vs), 947(s), 847(s), 792(s), 747(vs), 690(w), 656(s), 619(vs) cm^{-1}. Anal. Calcd. for $C_{15}H_{12}N_6$ (Mw = 276.30 g/mol): C, 65.21; H, 4.38; N, 30.42. Found: C, 64.55; H, 4.50; N, 29.97.

$Ni_3(BTP)_2\cdot 3DMF\cdot 5CH_3OH\cdot 17H_2O$ (1). Solid H_3BTP (500 mg, 1.81 mmol) was dissolved in DMF (50 mL) in a round-bottomed flask and $Ni(CH_3COO)_2\cdot 4H_2O$ (676 mg, 2.72 mmol) was added to the stirred solution. The mixture was heated at reflux for 16 h, with formation of a yellow precipitate observed in the first 4 h. Upon cooling, the yellow solid was collected by filtration, washed with methanol (3 × 10 mL) and dried under reduced pressure to yield 1.02 g (80%) of product. Anal. Calcd. for $C_{44}H_{93}N_{15}Ni_3O_{25}$ (Mw = 1408.37 g/mol): C, 37.52; H, 6.66;

N, 14.92. Found: C, 37.66; H, 5.75; N, 14.35. IR (neat): 3370(br), 1655(s), 1609(vs), 1557(w), 1406(w), 1385(w), 1361(w), 1329(w), 1257(s), 1196(w), 1135(w), 1078(vs), 1015(s), 854(w), 761(vs), 685(w), 640(s), 461(w) cm^{-1}.

$Ni_3(BTP)_2 \cdot 3CH_3OH \cdot 10H_2O$ (1m). A methanol-exchanged form of **1** was obtained by heating the solid immersed in methanol (10 mL) at 180 °C in a PTFE sealed pressure vessel for three days. Upon cooling, the precipitate was collected by filtration, washed with methanol (3 × 5 mL) and dried under reduced pressure for 12 h. Anal. Calcd. for $C_{33}H_{50}N_{12}Ni_3O_{13}$ (Mw = 998.90 g/mol): C, 39.68; H, 5.05; N, 16.83. Found: C, 39.53; H, 4.32; N, 16.60. IR (neat): 3365(br), 1609(vs), 1556(w), 1407(w), 1329(w), 1257(s), 1196(w), 1135(w), 1078(s), 1014(vs), 852(w), 761(vs), 686(w), 640(s), 462(w) cm^{-1}. The desolvated form of the compound (**1d**) was generated by heating **1m** under dynamic vacuum at 250 °C, as described below.

$Cu_3(BTP)_2 \cdot 8CH_3OH \cdot 10H_2O$ (2). A solution of H_3BTP (200 mg, 0.725 mmol) in 25 mL of DMF was added to a round-bottomed flask, together with $Cu(CH_3COO)_2 \cdot H_2O$ (186 mg, 0.930 mmol). The mixture was stirred and heated at 150 °C for 16 h, during which time a brown solid precipitated. Upon cooling, the solid was collected by filtration and suspended in 5 mL of methanol for 2 h. The brown solid was then collected by filtration, washed with methanol (3 × 10 mL) and dried under reduced pressure for 12 h to yield 320 mg (75%) of product. Anal. Calcd. for $C_{38}H_{70}Cu_3N_{12}O_{18}$ (Mw = 1173.70 g/mol): C, 38.89; H, 6.01; N, 14.32. Found: C, 38.56; H, 5.23; N, 14.66. IR (neat): 3370(br), 1608(vs), 1557(w), 1426(w), 1385(w), 1354(w), 1322(w), 1243(w), 1180(w), 1126(s), 1061(vs), 1012(vs), 946(w), 832(s), 758(vs), 681(w), 637(w), 460(w) cm^{-1}. The desolvated form of the compound (**2d**) was generated by heating **2** under dynamic vacuum at 250 °C, as described below.

$Cu_3(BTP)_2 \cdot 6H_2O$ (2′). Compound **2** (100 mg) was suspended in an aqueous HCl solution (10 mL, pH 3). The mixture was heated at 100 °C for one day in a 25-mL Teflon-capped scintillation vial. The dark brown suspension was then collected by filtration and washed with successive aliquots of water (3 × 10 mL) and methanol (3 × 5 mL). The same compound can be obtained by heating **2** in aqueous NaOH solution (10 mL, pH 14). Anal. Calcd. for $C_{30}H_{30}Cu_3N_{12}O_6$ (Mw = 845.27 g/mol): C, 42.63; H, 3.58; N, 19.88. Found: C, 42.69; H, 2.28; N, 19.23. IR (neat): 3130(br), 1679(w), 1610(s), 1593(vs), 1544(w), 1378(w), 1346(w), 1324(s), 1249(w), 1183(w), 1122(s), 1060(vs), 1043(w), 998(s), 942(w), 839(vs), 753(vs), 684(w), 643(s), 533(br), 456(w) cm^{-1}.

$Zn_3(BTP)_2 \cdot 4CH_3OH \cdot 2H_2O$ (3). H_3BTP (250 mg, 0.906 mmol) and $Zn(CF_3SO_3)_2$ (500 mg,

1.38 mmol) were dissolved in 30 mL of DMF in a round-bottomed flask, and the yellow solution was heated to 60 °C. Triethylamine (500 μL) was then added dropwise to the solution under vigorous stirring. Formation of a white precipitate was immediately observed. The mixture was then heated at reflux for 16 h. Upon cooling, the white solid was collected by filtration, washed with methanol (4 × 10 mL), and dried under vacuum to yield 320 mg (78%) of product. Anal. Calcd. for $C_{34}H_{38}N_{12}O_6Zn_3$ (Mw = 906.91 g/mol): C, 44.03; H, 4.22; N, 18.53. Found: C, 44.56; H, 3.98; N, 17.92. IR (neat): 3270(br), 1679(w), 1616(s), 1557(w), 1378(w), 1352(w), 1318(s), 1258(w), 1244(w), 1177(w), 1158(w), 1123(w), 1061(vs), 1009(s), 877(w), 845(s), 759(vs), 700(w), 677(w), 653(w) cm^{-1}.

$Zn_{12}[Zn_2(H_2O)_2]_6(BTP)_{16}$ (3′). Compound **3** (100 mg, 0.1103 mol) was suspended in an aqueous NaOH solution (10 mL, pH 14) in a 25-mL Teflon-capped scintillation vial and stirred at room temperature for 1 h. The white solid was then collected by filtration, and washed with water (3 × 10 mL) and methanol (3 × 5 mL). Anal. Calcd. For $C_{240}H_{168}N_{96}O_{12}Zn_{24}$ (Mw = 6157.90 g/mol): C, 46.81; H, 2.75; N, 21.84. Found: C, 45.91; H, 3.05; N, 19.95. IR (neat): 3603(w), 3300(br), 3112 (w), 1604(s), 1550(w), 1376(w), 1312(s), 1260(w), 1241(w), 1165(w), 1060(vs), 1004(s), 933(w), 847(vs), 753(vs), 695(w), 671(w), 656(w), 581(w), 544(br) cm^{-1}.

$Co_3(BTP)_2 \cdot 8CH_3OH \cdot 10H_2O$ (4). Under an N_2 atmosphere, H_3BTP (100 mg, 0.362 mmol) and $Co(CF_3SO_3)_2$ (194 mg, 0.543 mmol) were dissolved in 10 mL of DMF in a two-neck round-bottomed flask equipped with condenser and nitrogen inlet. The resulting purple solution was heated to 60 °C and triethylamine (250 μL) was added while hot. A deposit of dark purple solid immediately appeared. The mixture was then allowed to react for 16 h at reflux. Upon cooling, the solid was collected by filtration under nitrogen, washed with methanol (4 × 10 mL), and dried under vacuum to afford 150 mg (72%) of product as a purple powder. Anal. Calcd. For $C_{38}H_{70}Co_3N_{12}O_{18}$ (Mw = 1159.83 g/mol): C, 39.35; H, 6.08; N, 14.49. Found: C, 38.56; H, 5.98; N, 14.66. IR (neat): 3280(br), 1678(w), 1610(s), 1558(w), 1373(w), 1350(w), 1314(s), 1236(w), 1172(w), 1154(s), 1119(w), 1056(vs), 1042(s), 1007(s), 877(w), 843(s), 760(vs), 700(w), 675(w), 654(w) cm^{-1}.

Chemical Stability Tests. Compounds **1-3** (100 mg) were suspended in water in a 25-mL Teflon-capped scintillation vial and stirred at 100 °C for two weeks. At different time intervals (1 hour, 1 day, 3 days, 1 week, 2 weeks) an aliquot of each sample was collected by filtration, washed with successive aliquots of water (3 × 10 mL) and methanol (3 × 5 mL), dried under vacuum, and analyzed by X-ray powder diffraction. The same procedure was applied to the

stability tests in acidic (aqueous HCl or HNO_3, pH 2) and basic media (aqueous NaOH, pH 14).

Gas Sorption Measurements. Gas sorption isotherms for pressures in the range of 0-1.2 bar were measured by the volumetric method using an ASAP2020 analyzer (Micrometrics Instruments Corp., Norcross, GA) and the following procedure. A sample of ca. 100 mg of as-synthesized compound was transferred to a pre-weighed analysis tube (0.5-inch diameter, 10 cm^3 bulb), which was capped with a gas-tight transeal to prevent intrusion of oxygen and atmosphere moisture during transfer and weighing. The samples were evacuated under dynamic vacuum at 250 °C until an outgas rate of less than 2 mTorr/min (0.27 Pa/min) was achieved (2 days). The analysis tube containing the desolvated sample was then carefully transferred to an electronic balance and weighed again to determine the mass of the sample. It was then transferred back to the analysis port of the gas sorption instrument. The outgas rate was again confirmed to be less than 2 mTorr/min. For all isotherms, warm and cold free space correction measurements were performed using ultra high purity He gas (UHP grade 5.0, 99.999% purity); N_2 isotherms at 77 K were measured in a liquid nitrogen bath using UHP-grade gas sources.

Powder X-Ray Diffraction Structure Analysis. Microcrystalline samples were gently ground using an agate mortar and pestle, and were deposited in the hollow of an aluminum sample holder equipped with a zero-background plate. Diffraction data were collected by means of overnight scans in the 2θ range of 5-105° with 0.02° steps using a Bruker AXS D8 Advance diffractometer equipped with Ni-filtered Cu-Kα radiation (λ = 1.5418 Å), a Lynxeye linear position-sensitive detector, and mounting the following optics: primary beam Soller slits (2.3°), fixed divergence slit (0.3°), receiving slit (8 mm). The nominal resolution for the present set-up is 0.08° of 2θ (FWHM of the α_1 component) for the LaB_6 peak at about 2θ = 21.3°. The generator was set at 40 kV and 40 mA. A visual inspection of the acquired diffractograms revealed isomorphism between **1**, **1m**, **2**, and Mn-BTT,[3] as well as between **3** and **4**.

As a representative example of the nickel compounds, **1m** was chosen for a complete structural study. A standard peak search, followed by indexing through the Single Value Decomposition approach,[4] as implemented in TOPAS-R,[5] allowed the determination of approximate unit cell parameters. Space groups were assigned on the basis of the systematic absences, taking into consideration, when sensible, the purported isomorphism. Unit cells and space groups were checked by Le Bail refinements and later confirmed by successful structure solutions and refinements. For **1m**, **3**, and **3′**, structure solutions were performed by the simulated annealing technique, as implemented in TOPAS, employing a rigid, idealized model for the crystallographic independent portion of the BTP^{3-} ligand;[6] when sensible, the arene-pyrazole torsion was allowed to refine. It is worth noting that **1m** (as well as **1** and **2**) are *isomorphous*,

but not *isostructural*, to Mn-BTT,[3] thus requiring an independent structure solution process to retrieve their structural features. For **2** and **4**, a Rietveld refinement process was directly carried out starting from the structural models of their isostructural counterparts **1m** and **3**, respectively.

In both **1m** and **2**, the difference Fourier map calculated with the F_cs of the framework alone revealed that the solvent is highly disordered, either as guest molecules within the octahedral cavities or one-dimensional channels (see below), or covalently bound to the metal ions. Thus, its electronic density was modeled by allocating: (i) two dummy atoms at the centre of the cavities (site [½, ½, ½]) and of the channels (site [½, 0, 0]) and (ii) one dummy atom occupying, at a restrained distance, the apical position of the square pyramidal stereochemistry of the metal ions. The presence of disorder was taken into account by assigning to the three dummy atoms a high isotropic thermal parameter. Their site occupancy factors were allowed to refine up to the total electron density of the solvent, as estimated from the elemental analysis. In the cases of **3** and **4**, it was also not possible to locate the solvent in a definite position. Thus, the same approach as for **1m** and **2** was adopted, allocating one dummy atom within the cavities. The final refinements were carried out by the Rietveld method, maintaining the rigid bodies introduced at the structure solution stage. The background was modeled by a polynomial function. Peak shapes were described by the Fundamental Parameters Approach.[7] Anisotropic peak broadening was modeled using spherical harmonics to define the peak widths in the case of compounds **3** and **4**. A single, refined isotropic thermal parameter was assigned to each metal atom, and this was augmented by 2.0 $Å^2$ for the atoms of the BTP^{3-} ligand. Preferred orientation was modeled by using the March-Dollase approach along the [111] direction for compounds **1m** and **2**, and along the [001] direction for **3** and **4**. The final Rietveld refinement plots are shown in Figures S2-S4. It is worth noting that the still imperfect agreement between the experimental and the calculated traces in the case of **3′** is reasonably due to the fact that the positional disorder affecting the Zn2/O atoms (see Figure S5 and the crystal structure description) intrinsically induces disorder of the pyrazolate moieties, which cannot easily be modelled. Indeed, according to the atom present (Zn2 vs. O) and to its specific geometrical requirements (different for the Zn2-N and O-H···N bond distances) the pyrazolate rings may adopt two distinct orientations with respect to the central benzene ring, possibly forcing (locally) the whole ligand out from the crystallographic threefold axis. In spite of its high degree of crystallinity, we were unable to solve the structure of compound **2′**; hence, only the unit cell parameters and space group are available. X-ray crystallographic data of **1m**, **2**, **3**, **3′** and **4** CIF format have been deposited with the Cambridge Crystallographic Data Center as supplementary publications no.s 804989 - 804993. Copies of the data can be obtained free of charge on application to the Director, CCDC, 12 Union Road, Cambridge, CB2 1EZ,

UK (Fax: +44-1223-335033; e-mail: deposit@ccdc.cam.ac.uk or http://www.ccdc.cam.ac.uk). Relevant crystallographic data for species 1m, 2, 3, 4, 2' and 3' are collected on Table S1.

Thermodiffractometric Studies. Variable-temperature powder X-ray diffraction experiments were performed on the solvated compounds **1m**, **2**, **3**, and ***3′*** to probe their structural response to temperature increases. The experiments were carried out in air using a custom-made sample heater, assembled by Officina Elettrotecnica di Tenno, Ponte Arche, Italy. Powdered microcrystalline samples of the compounds were pulverized using an agate mortar and pestle, and were deposited in the hollow of an aluminum sample holder. Typically, the thermodiffractometric experiments were planned on the basis of the thermogravimetric analyses. The diffractograms were recorded in a significant low-angle 2θ range, heating *in situ* by increments of 30 °C, starting from 30 °C, until significant loss of crystallinity was observed. Parametric treatment (using the Le Bail method) of the data acquired before loss of crystallinity revealed the unit cell parameter variations as a function of the temperature in the cases of **1m**, **2**, **3**, and ***3′***. When comparing the thermogravimetric and thermodiffractometric results, the reader should be aware that the thermocouple of the latter set up was *not* in direct contact with the sample, potentially leading to slight difference in the temperature at which the same event is detected by the two techniques. The temperatures obtained by thermogravimetric analysis should be considered more reliable.

Other Physical Measurements. ^{1}H-NMR spectra (in DMSO-d_6) were recorded at 298 K on a Bruker Avance 400 instrument (400 MHz) in the NMR Facility of the University of California, Berkeley. Elemental analyses were obtained from the Microanalytical Laboratory of the University of California, Berkeley. Infrared spectra were recorded on a Perkin Elmer Spectrum 100 Optica FTIR spectrometer. Thermogravimetric analyses were carried out at a ramp rate of 3 °C/min under nitrogen flow with a TA Instruments TGA Q5000. X-ray fluorescence analyses were performed with a Panalytical Minipal 2 instrument, equipped with a Cr source, on a powdered batch of **1**.

Table S1. Crystallographic data for species **1m**, **2**, **3**, **4**, **2′** and **3′**.

	1m	**2**	**3**	**4**	**2′**[a]	**3′**
Emp. Form.	$C_{33}H_{50}Ni_3N_{12}O_{13}$	$C_{38}H_{70}Cu_3N_{12}O_{18}$	$C_{34}H_{38}N_{12}O_6Zn_3$	$C_{38}H_{70}Co_3N_{12}O_{18}$	$C_{30}H_{30}Cu_3N_{12}O_6$	$C_{120}H_{84}N_{48}O_6Zn_{12}$
Mw, g mol^{-1}	998.9	1173.7	906.9	1159.8	845.3	3079.0
Crystal system	Cubic	Cubic	Tetragonal	Tetragonal	Rhombohedral	Cubic
Space group, Z	$Pm\bar{3}m$, 4	$Pm\bar{3}m$, 4	$P4_2/ncm$, 4	$P4_2/ncm$, 4	$R3c$	$Pn\bar{3}n$, 2
a, Å	18.5490(8)	18.8070(8)	15.555(1)	15.462(1)	23.794(6)	18.547(1)
b, Å						
c, Å			20.030(2)	20.047(2)	12.869(4)	
V, Å^3	6382.0(8)	6652.1(8)	4846.5(7)	4793(1)	6309(4)	6380(1)
ρ_{calc}, g/cm^3	1.04	1.13	1.20	1.55	n.a.	3096
F(000)	2080	2452	1856	2428	n.a.	1.60
μ(CuKα) cm^{-1}	14.62	16.50	21.33	87.93	n.a.	30.2
T, K	298(2)	298(2)	298(2)	298(2)	298(2)	298(2)
2θ range, °	5-105	5-105	5-105	5-105	5-105	5-105
N_{data}	5001	5001	5001	5001	5001	5001
R_{wp}, R_p	0.068, 0.042	0.103, 0.065	0.102, 0.072	0.119, 0.092	0.019, 0.013	0.156, 0.113
R_{Bragg}	0.028	0.028	0.040	0.037	n.a.	0.094

[a]The values reported for **2′** result from a structureless Le Bail refinement.

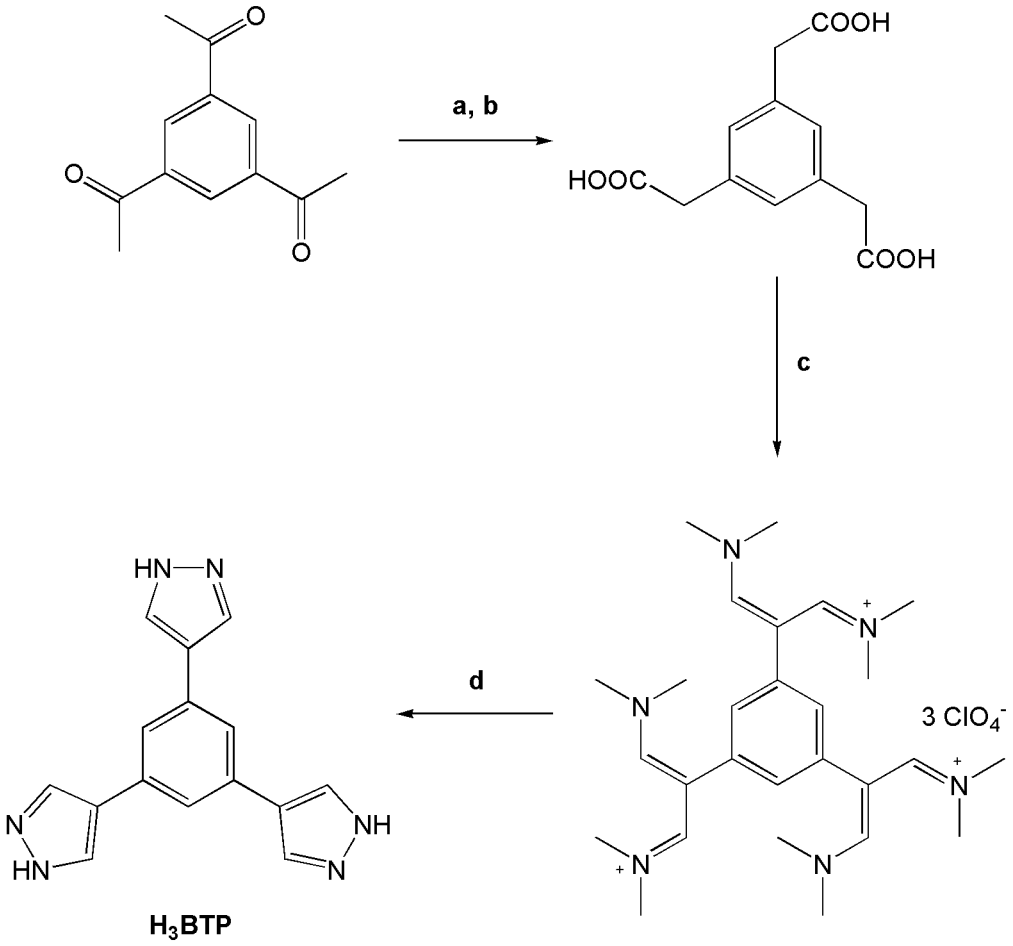

Figure S1. Schematic synthesis of 1,3,5-tris(1*H*-pyrazol-4-yl)benzene ligand (**H_3BTP**): a) S_8, morpholine, 120°C, 20h, than water; b) H_2SO_4 conc., CH_3COOH, H_2O 100 °C, 15h; c) $POCl_3$, DMF, 90°C, 15h than ice/H_2O, $NaClO_4$; d) $N_2H_4.H_2O$, ethanol, reflux, 3h.

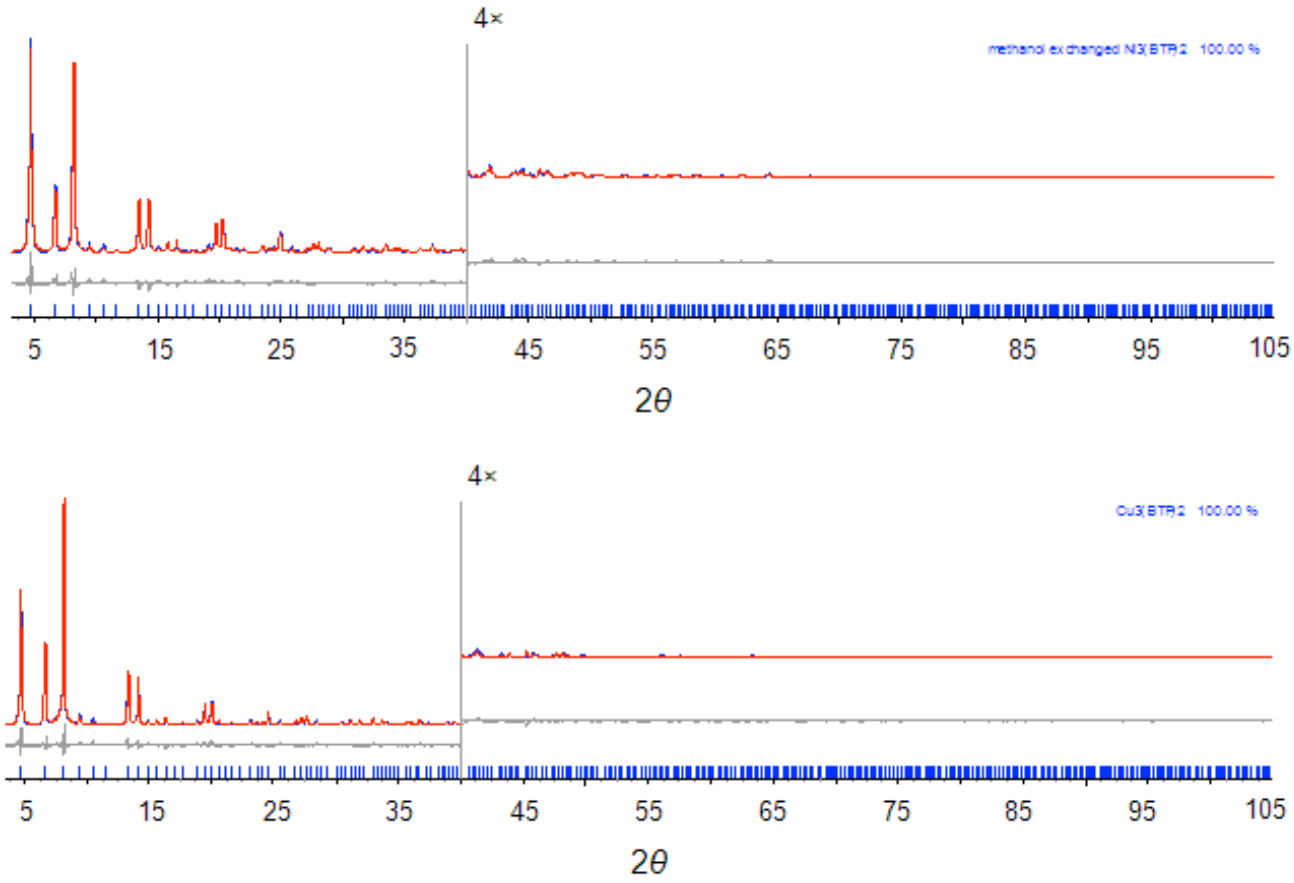

Figure S2: Rietveld refinement results for compounds **1m** (top) and **2** (bottom) in terms of experimental (blue), calculated (red) and difference (grey) diffraction traces. The peaks markers are shown at the bottom. The portion above 40 deg has been magnified (4×).

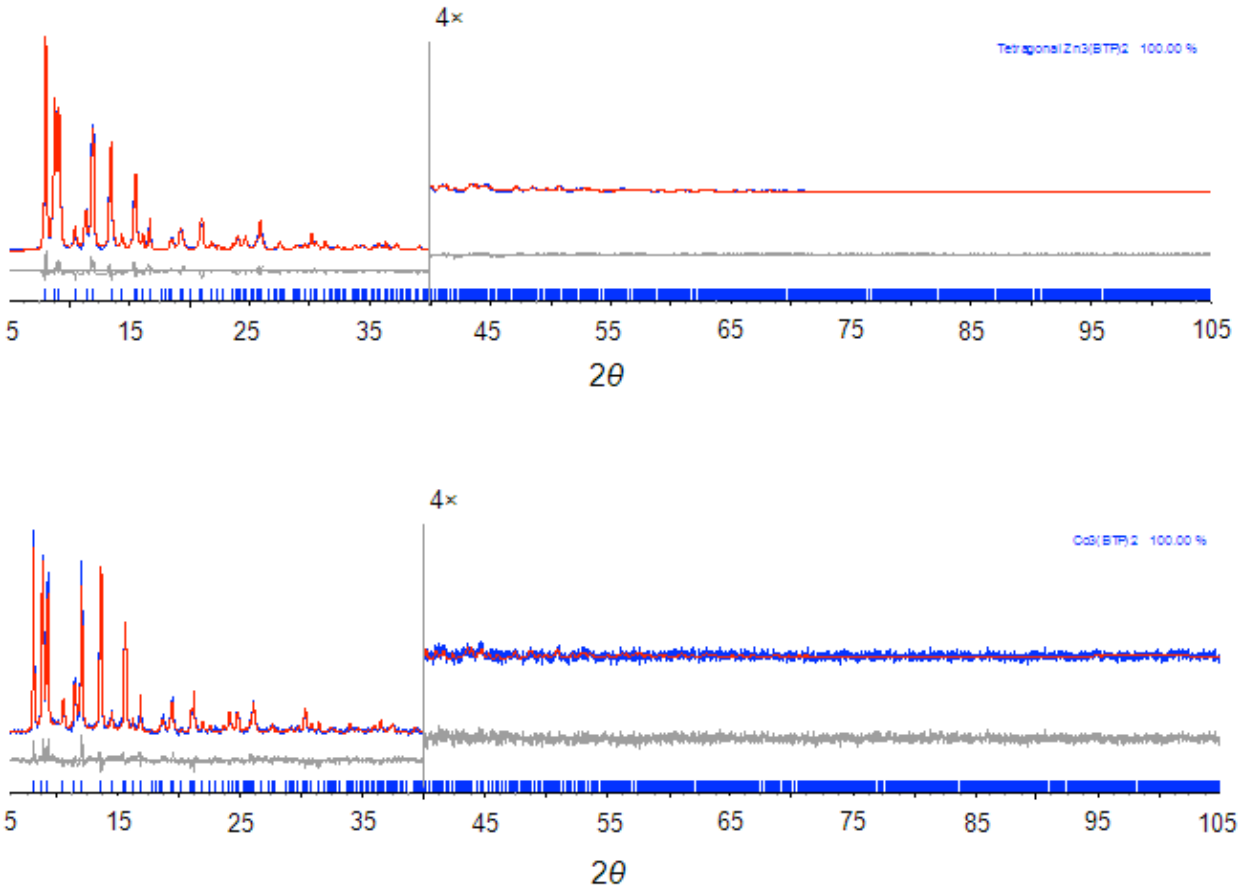

Figure S3: Rietveld refinement results for compounds **3** (top) and **4** (bottom) in terms of experimental (blue), calculated (red) and difference (grey) diffraction traces. The peaks markers are shown at the bottom. The portion above 40 deg has been magnified (4×).

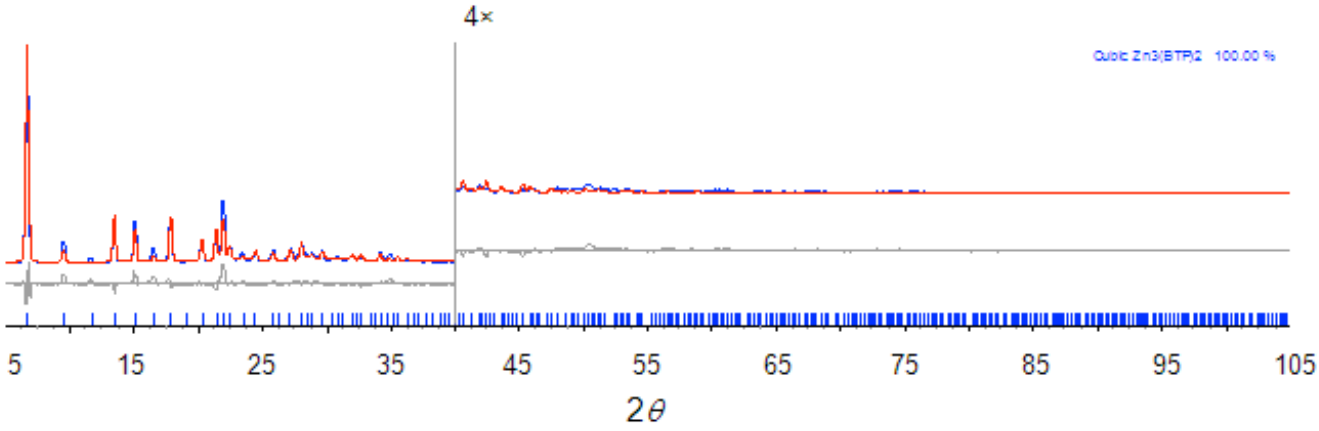

Figure S4: Rietveld refinement results for compounds **3′** of experimental (blue), calculated (red) and difference (grey) diffraction traces. The peaks markers are shown at the bottom. The portion above 40 deg has been magnified (4×). Please note that the limited agreement between the experimental and the calculated trace is reasonably due to the fact that the positional disorder affecting the Zn2/O couple (see Figure SX and the crystal structure description) may induce disorder of the pyrazolate moieties, which we cannot easily model. Indeed, according to the atom (Zn2 *vs* O) present, the pyrazolate rings reasonably adopt two distinct orientations with respect to the central benzene ring.

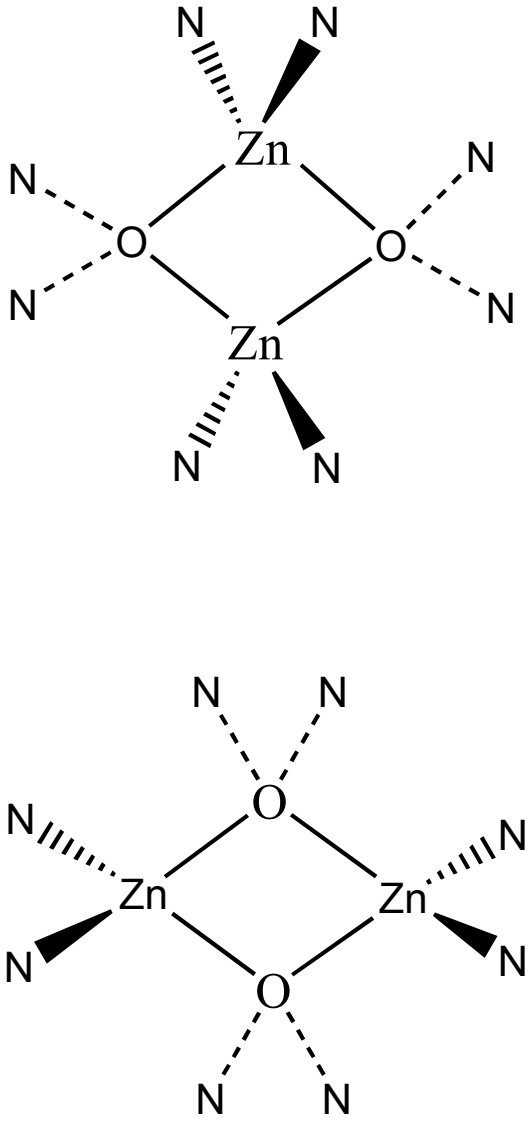

Figure S5. Schematic description of the local disorder affecting the $[Zn_2(H_2O)]_2$ fragment in ***3′***. The H atoms of the N---HO hydrogen bonds are omitted for clarity.

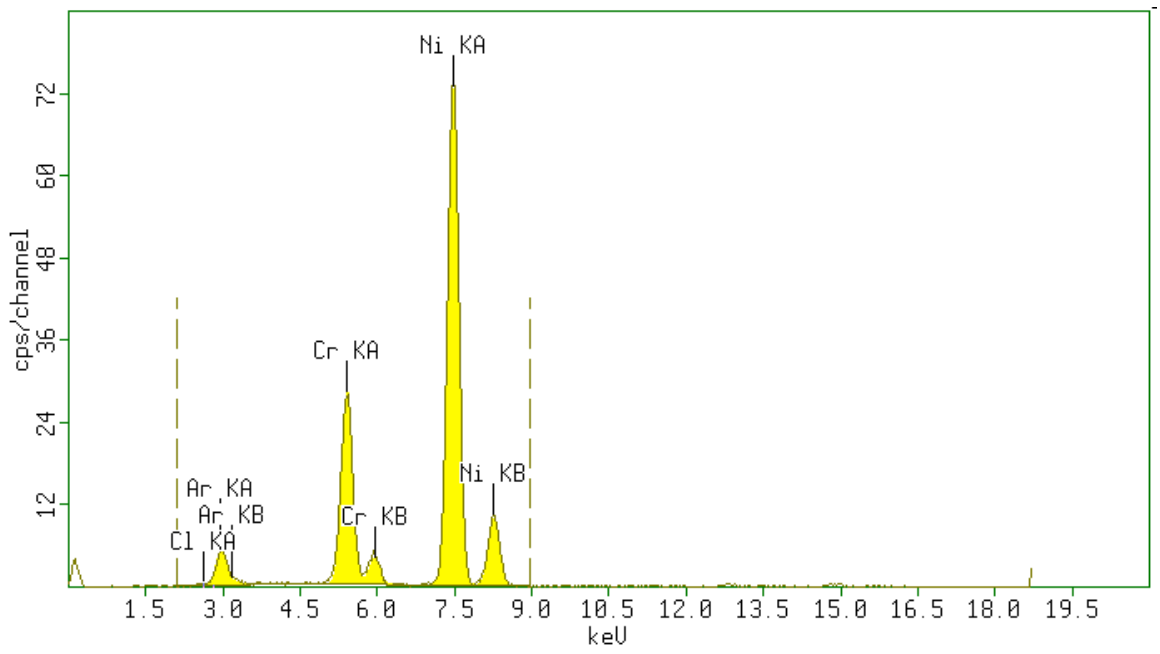

Figure S6. Qualitative X-Ray Fluorescence analysis of $Ni_3(BTP)_2 \cdot 3DMF \cdot 5CH_3OH \cdot 17H_2O$, **1**.

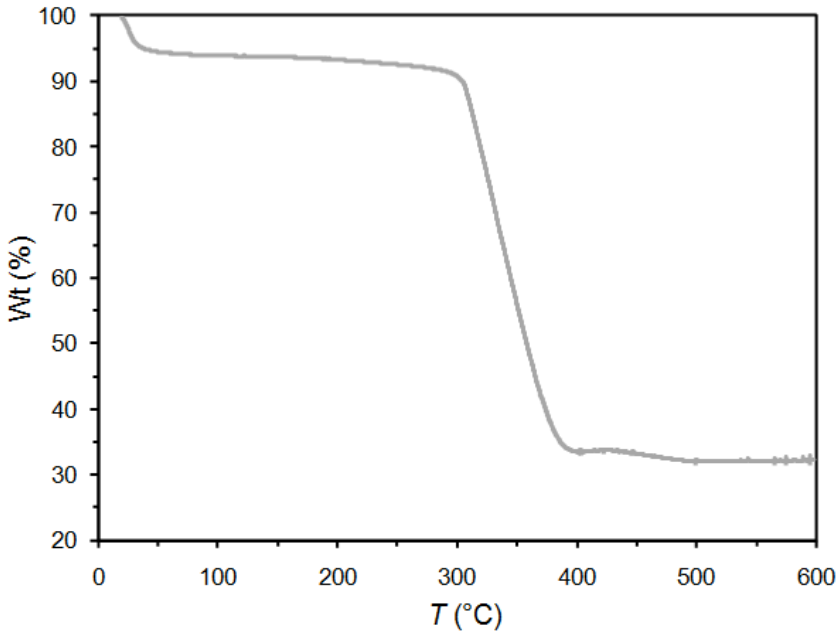

Figure S7. Thermal gravimetric analysis of as-synthesized $Cu_3(BTP)_2(H_2O)_6$, **2′**.

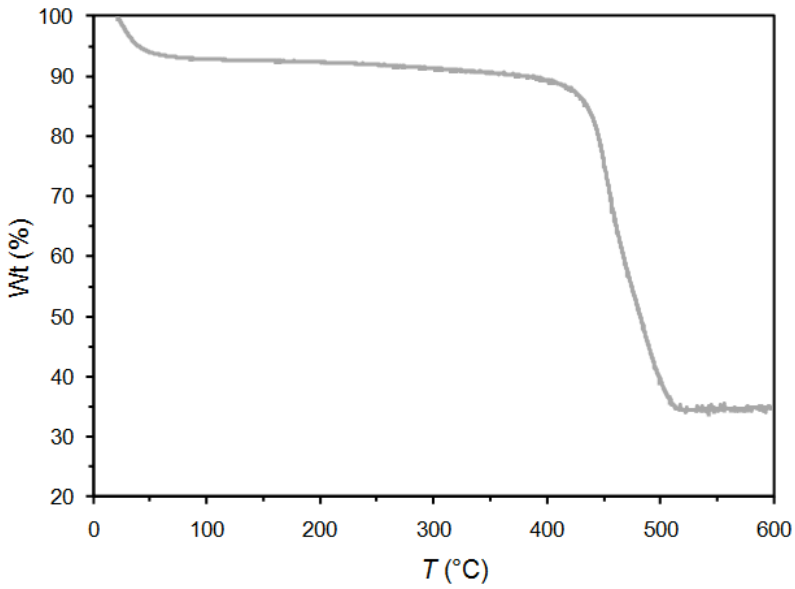

Figure S8. Thermal gravimetric analysis of as-synthesized $Zn_{12}[Zn_2(H_2O)_2]_6(BTP)_{16}$, ***3′***.

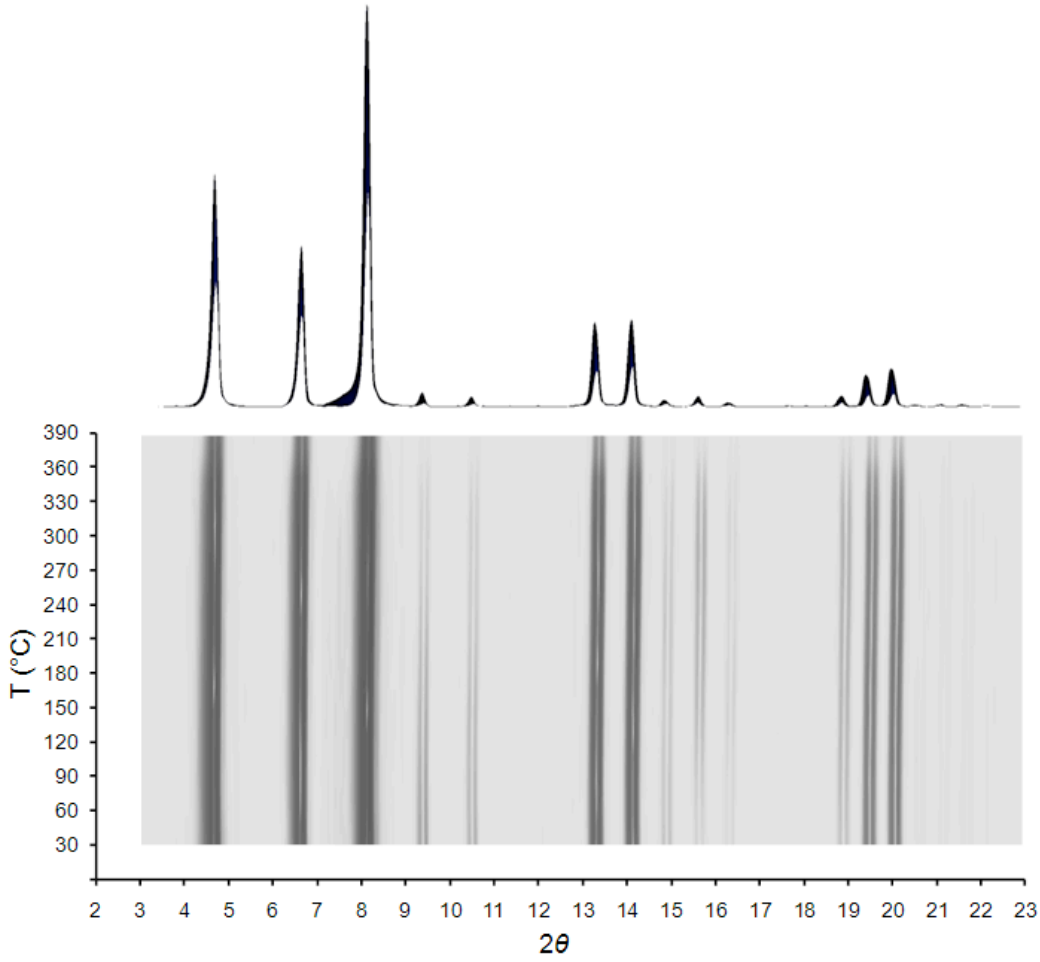

Figure S9. Bottom: 2D plot representing a series of diffractograms collected in variable temperature on the Cu_3BTP_2, **2**, sample. Horizontal axis, 2θ. Vertical axis, temperature range 30 - 390 °C. Top: front view of the same set of data showing framework rigidity.

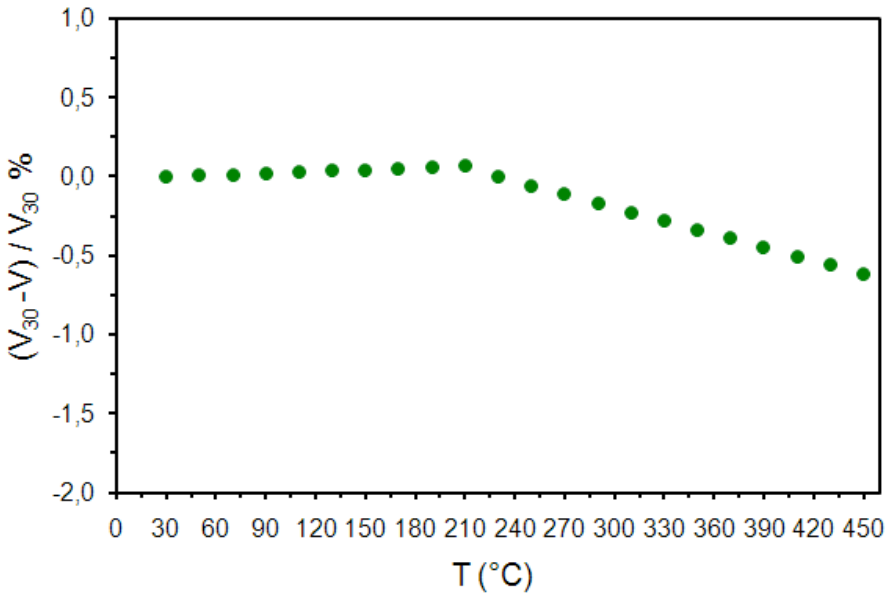

Figure S10. Variation of the unit cell volume of **1** (V) normalized to the corresponding 30 °C values (V_{30}) as a function of the temperature.

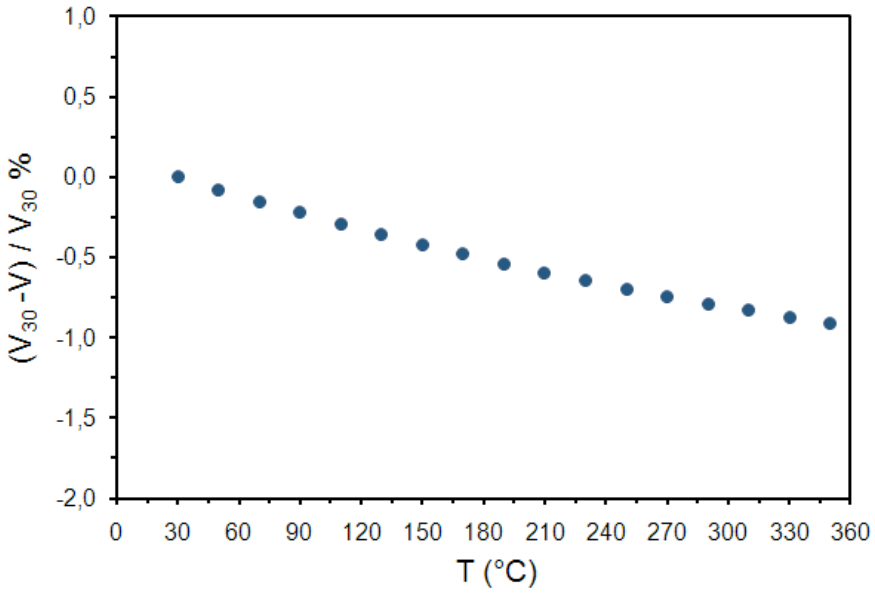

Figure S11. Variation of the unit cell volume of **2** (V) normalized to the corresponding 30 °C values (V_{30}) as a function of the temperature.

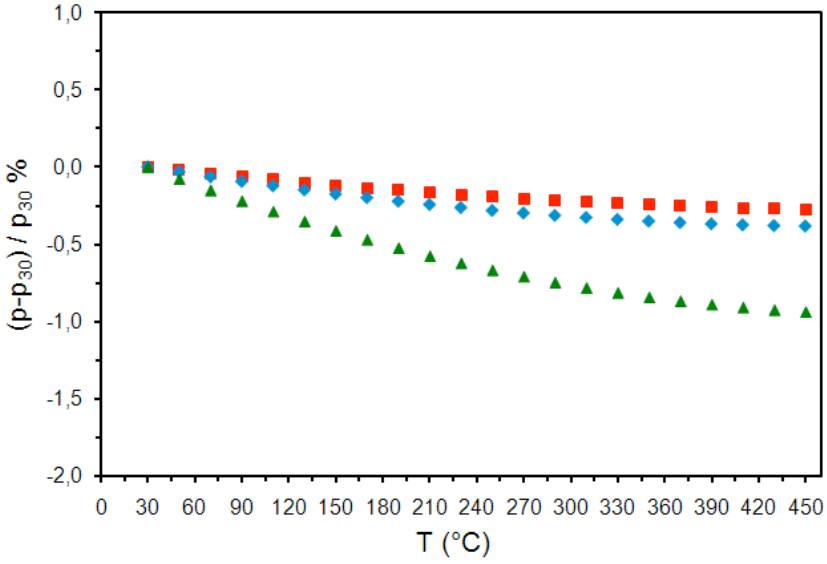

Figure S12. Variation of the unit cell parameters of **3** (p) normalized to the corresponding 30 °C values (p_{30}) as a function of the temperature. *a*, red squares; *c*, blue rhombi; *V*, green triangles.

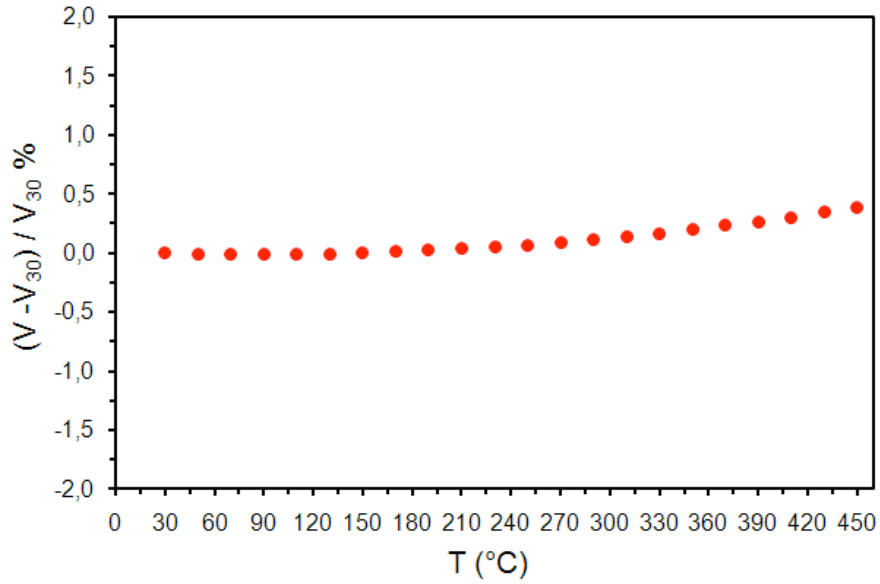

Figure S13. Variation of the unit cell volume of ***3′*** (V) normalized to the corresponding 30 °C values (V_{30}) as a function of the temperature.

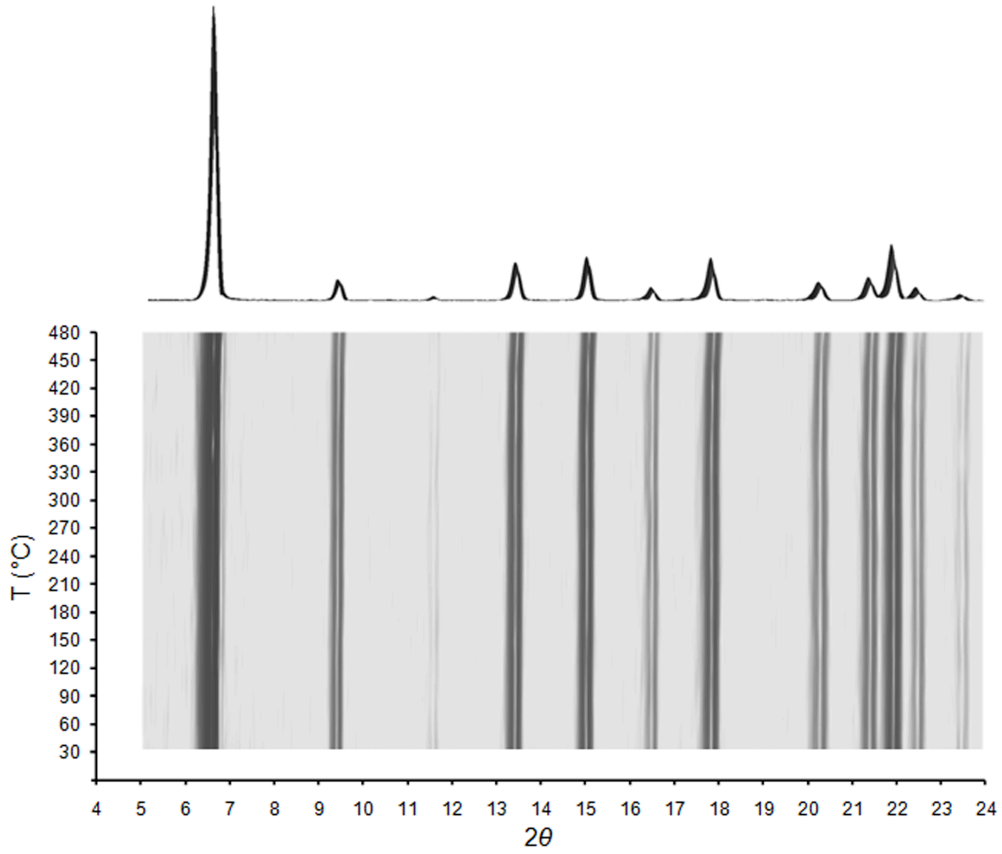

Figure S14. Bottom: 2D plot representing a series of diffractograms collected in variable temperature on the $Zn_{12}[Zn_2(H_2O)_2]_6(BTP)_{16}$, **3′**, sample. Horizontal axis, 2θ. Vertical axis, temperature range 30 - 390 °C. Top: front view of the same set of data showing framework rigidity.

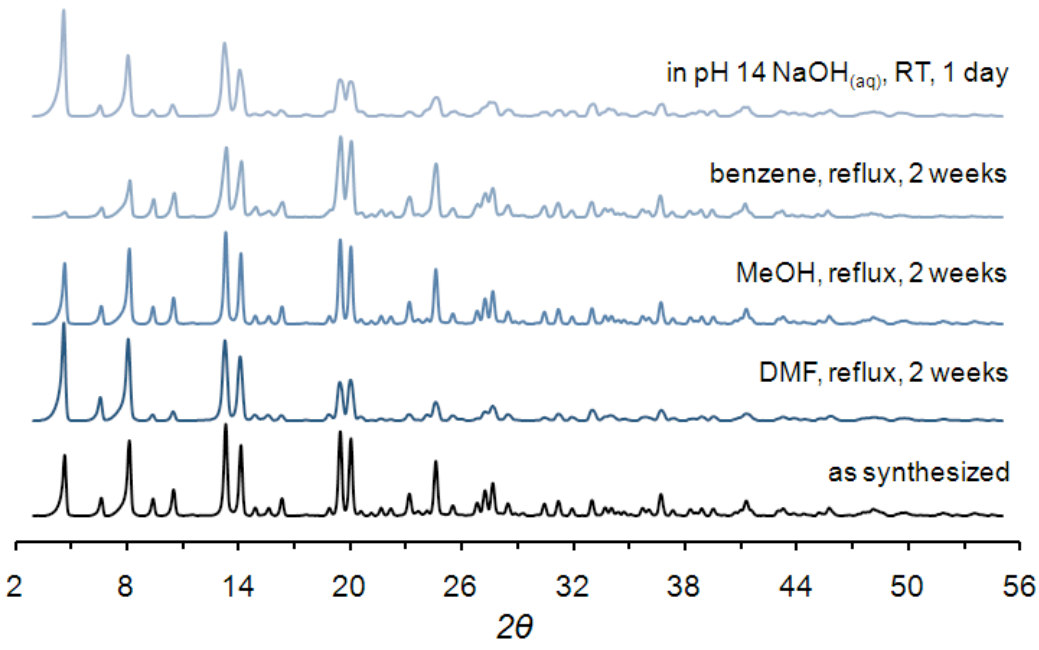

Figure S15. X-ray powder diffraction patterns of (bottom to top) $Cu_3(BTP)_2$ as-synthesized, **2**; after two weeks in DMF, MeOH and benzene at reflux and in a pH 14 of aqueous NaOH solution for 1 day at room temperature.

1 (a) M. S. Newmann and H. S. Lowrie, *J. Am. Chem. Soc.,* 1954, **76**, 6196. (b) R. Gompper, Gompper, C. Harfmann and K. Polborn, *J. Prakt. Chem.*, 1998, **340**, 381.

2 (a) V. Lozan, P. Solntsev, G. Leibiling, K. V. Domasevitch, B. Kersting, *Eur. J. Inorg. Chem.,* 2007, **46**, 3217. (b) A. Maspero, S. Galli, N. Masciocchi, G. Palmisano, *Chem. Lett.*, 2008, **37**, 956. (c) N. Masciocchi, S. Galli, V. Colombo, A. Maspero, G. Palmisano, B. Seyyedi, C. Lamberti, S. Bordiga, *J. Am. Chem. Soc.,* 2010, **132**, 7902.

3 (a) M. Dincă, A. Dailly, Y. Liu, C. M. Brown, D. A. Neumann and J. R. Long, J. Am. Chem. Soc., 2006, **128**, 16876.

4 A. Coelho, *Appl. Cryst.,* 2003, **36**, 86.

5 Version 3.0, Bruker AXS 2005, Karlsruhe, Germany.

6 To build the rigid model describing the ligand, the followind bond distances and angles have been adopted a) for the benzene ring: C-C = 1.39 Å; C-H = 0.95 Å; C-C-C, C-C-H = 120°; b) for the pyrazole ring: C-C, C-N, N-N = 1.36 Å; C-H = 0.95 Å; internal ring angles = 108°; C-C-H = 126°. Cbenzene-Cpyrazole = 1.45 Å.

7 R. W. Cheary, A. Coelho, *J. Appl. Cryst.,* 1998, **31**, 85; *ibid.* 862.